

Acceleration of Galactic Supershells by $\text{Ly}\alpha$ Radiation

Mark Dijkstra ^{*} and Abraham Loeb

Astronomy Department, Harvard University, 60 Garden Street, Cambridge, MA 02138, USA

11 November 2018

ABSTRACT

Scattering of $\text{Ly}\alpha$ photons by neutral hydrogen gas in a single outflowing ‘supershell’ around star forming regions often explains the shape and offset of the observed $\text{Ly}\alpha$ emission line from galaxies. We compute the radiation pressure that is exerted by this scattered $\text{Ly}\alpha$ radiation on the outflowing material. We show that for reasonable physical parameters, $\text{Ly}\alpha$ radiation pressure alone can accelerate supershells to velocities in the range $v_{\text{sh}} = 200\text{--}400 \text{ km s}^{-1}$. These supershells possibly escape from the gravitational potential well of their host galaxies and contribute to the enrichment of the intergalactic medium. We compute the physical properties of expanding supershells that are likely to be present in a sample of known high-redshift ($z = 2.7\text{--}5.0$) galaxies, under the assumption that they are driven predominantly by $\text{Ly}\alpha$ radiation pressure. We predict ranges of radii $r_{\text{sh}} = 0.1\text{--}10 \text{ kpc}$, ages $t_{\text{sh}} = 1\text{--}100 \text{ Myr}$, and energies $E_{\text{sh}} = 10^{53}\text{--}10^{55} \text{ ergs}$, which are in reasonable agreement with the properties of local galactic supershells. Furthermore, we find that the radius, r_{sh} , of a $\text{Ly}\alpha$ -driven supershell of constant mass depends uniquely on the intrinsic $\text{Ly}\alpha$ luminosity of the galaxy, L_{α} , the HI column density of the supershell, N_{HI} , and the shell speed, v_{sh} , through the scaling relation $r_{\text{sh}} \propto L_{\alpha}/(N_{\text{HI}}v_{\text{sh}}^2)$. We derive mass outflow rates in supershells that reach $\sim 10\text{--}100\%$ of the star formation rates of their host galaxies.

Key words: cosmology: theory–galaxies: high redshift–radiation mechanisms: general–radiative transfer–ISM: bubbles

1 INTRODUCTION

The $\text{Ly}\alpha$ emission line of galaxies is often redshifted relative to metal absorption lines (e.g. Pettini et al. 2001; Shapley et al. 2003). Scattering of $\text{Ly}\alpha$ photons by neutral hydrogen atoms in an outflowing ‘supershell’ surrounding the star forming regions can naturally explain this observation, as well as the typically observed asymmetric spectral shape of the $\text{Ly}\alpha$ emission line (Lequeux et al. 1995; Lee & Ahn 1998; Tenorio-Tagle et al. 1999; Ahn & Lee 2002; Ahn et al. 2003; Mas-Hesse et al. 2003; Ahn 2004; Verhamme et al. 2006, 2008). The presence of an outflow may also be required to avoid complete destruction¹ of the $\text{Ly}\alpha$ radiation by dust and to allow its escape from the host galaxies (Kunth et al. 1998; Hayes et al. 2008; Ostlin et al. 2008; Atek et al. 2008).

Indeed, the existence of outflowing thin shells (with a thickness much smaller than their radius) of neutral

atomic hydrogen around HII regions is confirmed by HI-observations of our own (Heiles 1984) and other nearby galaxies (e.g. Ryder et al. 1995). The largest of these shells, so-called ‘supershells’, have radii of $r_{\text{max}} \sim 1 \text{ kpc}$ (e.g. Ryder et al. 1995; McClure-Griffiths et al. 2002, 2006) and HI column densities in the range $N_{\text{HI}} \sim 10^{19}\text{--}10^{21} \text{ cm}^{-2}$ (e.g. Lequeux et al. 1995; Kunth et al. 1998; Ahn 2004; Verhamme et al. 2008). The existence of larger extragalactic supershells has been inferred from spatially extended (\sim a few kpc) $\text{Ly}\alpha$ P-cygni profiles, that were observed around local star burst galaxies (Mas-Hesse et al. 2003). These ‘supershells’ differ from more energetic ‘superwinds’ (e.g. Heckman et al. 1990; Martin 2005), in which galactic-scale biconical outflows break-out of the galaxies’ interstellar medium with high velocities (up to $\sim 10^3 \text{ km s}^{-1}$, of which M82 is a classical example). Supershells are thought to be generated by stellar winds or supernovae explosions which sweep-up gas into a thin expanding neutral shell (see e.g. Tenorio-Tagle & Bodenheimer 1988, for a review). The back-scattering mechanism attributes both the redshift and asymmetry of the $\text{Ly}\alpha$ line to the Doppler boost that $\text{Ly}\alpha$ photons undergo as they scatter off the outflow on the far side of the galaxy back towards the observer.

In this paper we show that the radiation pressure ex-

^{*} E-mail:mdijkstr@cfa.harvard.edu

¹ $\text{Ly}\alpha$ may also avoid complete destruction by interstellar dust when it is primarily locked up in cold clumps embedded in a hot medium that is transparent to $\text{Ly}\alpha$ (Neufeld 1991; Hansen & Oh 2006).

erted by backscattered Ly α radiation on the outflowing gas shell can accelerate it to velocities that reach hundreds of km s $^{-1}$. Our basic result can be illustrated through an order-of-magnitude estimate. The net outward force exerted on a shell of gas² by backscattered Ly α radiation of luminosity $L_{\text{BS},\alpha}$ is $d(m_{\text{sh}}v_{\text{sh}})/dt = L_{\text{BS},\alpha}/c$. Here, m_{sh} is the total mass in the shell, v_{sh} is the shell velocity and c is the speed of light. If we assume that backscattering occurs over a timescale t_{BS} , and the shell mass is constant in time, then the net velocity gain by the shell is $\Delta v_{\text{sh}} \sim 250 \text{ km s}^{-1} (m_{\text{sh}}/10^7 M_{\odot})^{-1} (t_{\text{BS}}/50 \text{ Myr}) (L_{\text{BS},\alpha}/10^{43} \text{ erg/s})$. The adopted m_{sh} value corresponds to a thin spherical HI shell with a column density $N_{\text{HI}} = 10^{20} \text{ cm}^{-2}$ and radius $r = 1 \text{ kpc}$. The fiducial values of $L_{\text{BS},\alpha}$ and t_{BS} were chosen to yield the typical observed shell speed and expected shell lifetime in Lyman-break galaxies (LBGs; see e.g. Shapley et al. 2003; Verhamme et al. 2008). Here, and throughout this paper, we assume that the supershells are mostly neutral. This assumption is based on 21-cm observations of local supershells which indicate that these are very thin (thickness \ll their radius, e.g. Heiles 1984) and therefore dense. At these high densities one expects free electrons and protons to recombine efficiently and make the gas significantly neutral. However, Pettini et al. (2000) argue that, based on the observed reddening of the UV continuum spectrum, either the dust-to-gas ratio in the supershell of LBG MS1512-cB58 is higher than the galactic value, or alternatively that the HI only makes up $f_{\text{HI}} \sim 14 - 33\%$ of the total gas mass of the shell, with the remainder of the gas being molecular or ionized. We discuss how this latter possibility affects our results in § 3.

This paper is a closely related to another paper in which detailed Monte-Carlo Ly α radiative transfer calculations are performed to assess Ly α radiation pressure in a more general context (Dijkstra & Loeb 2008, hereafter Paper I). These radiative transfer calculations illustrate clearly that Ly α radiation pressure may be important in driving outflows in various environments. Importantly, the pressure exerted by Ly α radiation alone can exceed the maximum possible pressure exerted by continuum radiation through dust opacity (see Paper I), which in turn can exceed the total kinetic pressure exerted by supernova ejecta (Murray et al. 2005). This implies that Ly α radiation pressure may thus in some cases provide the dominant source of pressure on neutral hydrogen gas in the interstellar medium (ISM).

The goals of this paper are (i) to gauge the general importance of Ly α radiation in the particular context of outflowing galactic supershells, and (ii) to explore the related observable properties of Ly α -driven supershells. In § 2 we compute the time evolution of the velocity of an expanding

shell of neutral gas that encloses a central Ly α source. We consider a range of models, which are subsequently applied to known Ly α emitting galaxies at high redshifts. Finally, we discuss our results and their implications in § 3. The parameters for the background cosmology used throughout our discussion are $(\Omega_m, \Omega_{\Lambda}, \Omega_b, h) = (0.27, 0.73, 0.042, 0.70)$ (Dunkley et al. 2008; Komatsu et al. 2008).

2 PRESSURE FROM BACKSCATTERED LY α RADIATION

As mentioned in § 1, the net momentum transfer rate from the Ly α radiation field to the shell is given by

$$\frac{d(m_{\text{sh}}v_{\text{sh}})}{dt} = m_{\text{sh}} \frac{dv_{\text{sh}}}{dt} = f_{\text{scat}}(v_{\text{sh}}, N_{\text{HI}}) \frac{L_{\alpha}}{c}, \quad (1)$$

where L_{α} is the total Ly α luminosity of the galaxy, and $f_{\text{scat}}(v_{\text{sh}}, N_{\text{HI}})$ denotes the fraction of Ly α photons that are scattered in the shell. The latter depends on various factors, including the column density of neutral hydrogen atoms in the shell, the intrinsic Ly α spectrum (i.e. the emitted spectrum *prior* to scattering in the shell), as well as the shell velocity. For example, as v_{sh} increases, atoms in the shell interact with Ly α photons that are farther in the wing of the line profile, and f_{scat} diminishes. Eq. 1 assumes that the HI shell mass remains constant in time. This assumption is motivated by the observation that supershells are well defined shells of HI gas that are physically separate from the central Ly α source. These outflows differ from steady-state outflows (i.e. outflows in which mass is ejected at a constant rate \dot{M}) that occur around late-type stars (e.g. Salpeter 1974; Ivezić & Elitzur 1995). In reality, an HI supershell is not likely to maintain a constant mass as it sweeps through the ISM, but its evolution depends on the detailed hydrodynamics of the shell as it propagates through the ISM, which in turn depends on the assumed properties of the ISM. In this first study, we focus on simplified models that gauge the general importance of Ly α radiation pressure on the dynamics of galactic supershells.

Furthermore, our calculation of the parameter f_{scat} conservatively ignores that possibility of ‘trapped’ Ly α photons by the expanding supershell, which can boost the radiation pressure considerably. If radiation trapping were included, then the parameter f_{scat} would equal the ‘force-multiplier’ M_F , which was shown to be much greater than unity at low v_{sh} in Paper I (see § 3 for a more detailed discussion). We adopt a conservative approach because the calculation of M_F in Paper I assumed that the expanding shell contained no dust. Under realistic circumstances, the existence of dust inside the supershell will suppress the number of times the Ly α photons can ‘bounce’ back and forth between opposite sites of the shell, which leads to a reduction in the value of M_F . However, provided that the dust is located inside (or exterior to) the HI shell, the true value of M_F is always larger than the f_{scat} adopted in the paper (see § 3).

2.1 Calculation of f_{scat}

We compute $f_{\text{scat}}(v_{\text{sh}}, N_{\text{HI}})$ under the conventional set of assumptions: (i) the emitted Ly α spectrum prior to scattering is assumed to be a Gaussian with a velocity width

² The net momentum transfer rate per photon that enters the shell is $\Delta \mathbf{p} = \frac{h\nu_{\alpha}}{c} (1 - \mu) \mathbf{e}_r$, where \mathbf{e}_r denotes a unit vector that is pointing radially outward. Furthermore, $\mu = \mathbf{k}_{\text{in}} \cdot \mathbf{k}_{\text{out}}$, where \mathbf{k}_{in} (\mathbf{k}_{out}) denotes the propagation direction of the Ly α photon as it enters (leaves) the shell. When averaged over all directions, the total momentum transfer rate is $\dot{N}_{\alpha} \frac{h\nu_{\alpha}}{c} \mathbf{e}_r$, where \dot{N}_{α} is the rate at which Ly α photons enter the shell. This total net momentum transfer rate applies regardless of the number of times each Ly α photon scatters inside the shell, or regardless of whether the Ly α photon is absorbed by a dust grain (and possibly re-emitted in the infrared).

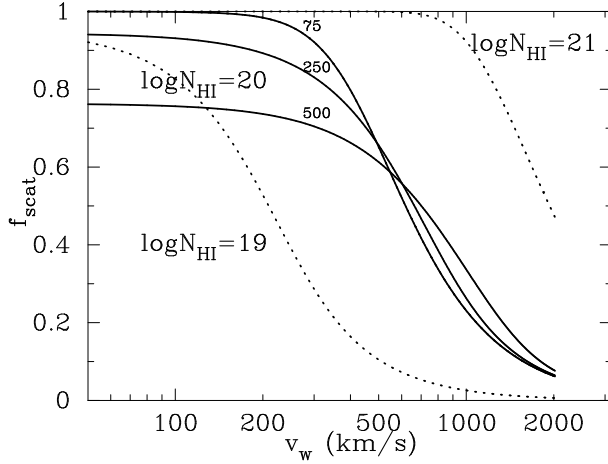


Figure 1. The fraction of scattered Ly α photons f_{scat} as a function of shell velocity v_{sh} for a range of column densities N_{HI} (in cm^{-2} , for $\sigma = 75 \text{ km s}^{-1}$) and emitted line widths quantified by σ (labeled by 75, 250 and 500 km s^{-1} for $\log N_{\text{HI}} = 20$). Higher N_{HI} values require larger shell speeds in order for the Ly α photons to propagate through the shell unobscured, because as N_{HI} increases the photons need to be farther in the wing of the line profile (in the frame of the shell) for them not to scatter. Furthermore, a larger intrinsic line width, σ , serves to flatten the dependence of f_{scat} on the shell speed (see text).

$\sigma = v_{\text{circ}}$ (Santos 2004; Dijkstra et al. 2007), where v_{circ} is the circular virial velocity of the host dark matter halo; and (ii) the outflow is modeled as a single expanding thin shell of gas with a column density N_{HI} (as in Ahn et al. 2003; Ahn 2004; Verhamme et al. 2006, 2008). We can then write

$$f_{\text{scat}}(v_{\text{sh}}, N_{\text{HI}}) = \frac{1}{\sqrt{2\pi}\sigma_x} \int dx e^{-x^2/2\sigma_x^2} e^{-N_{\text{HI}}\sigma_\alpha(x-x_{\text{sh}})}, \quad (2)$$

where frequency is denoted by the dimensionless variable $x \equiv (\nu - \nu_0)/\Delta\nu_D$, with $\Delta\nu_D = v_{\text{th}}\nu_0/c$ and v_{th} being the thermal velocity of the hydrogen atoms in the gas given by $v_{\text{th}} = \sqrt{2k_B T/m_p}$, k_B is the Boltzmann constant, $T = 10^4 \text{ K}$ is the gas temperature, m_p is the proton mass, $\nu_0 = 2.47 \times 10^{15} \text{ Hz}$ is the Ly α resonance frequency, $\sigma_x = \sigma/v_{\text{th}}$, and $x_{\text{sh}} = v_{\text{sh}}/v_{\text{th}}$. In Figure 1 we show f_{scat} as a function of v_{sh} for a range of column densities N_{HI} (for $\sigma = 75 \text{ km s}^{-1}$) and emitted line widths σ (for $N_{\text{HI}} = 10^{20} \text{ cm}^{-2}$).

As illustrated in Figure 1, f_{scat} increases with increasing N_{HI} , because photons need to be farther in the wing of the line profile (in the frame of the shell) for them not to scatter. For example, Figure 1 shows that $\sim 50\%$ of the Ly α photons are scattered when the shell speed is $\sim 200 \text{ km s}^{-1}$ for $N_{\text{HI}} = 10^{19} \text{ cm}^{-2}$, whereas the same fraction is reached when the shell speed is ~ 600 (2000) km s^{-1} for $N_{\text{HI}} = 10^{20}$ ($N_{\text{HI}} = 10^{21}$) cm^{-2} . Furthermore, increasing the intrinsic line width serves to flatten the dependence of f_{scat} on the shell speed, because at large σ and low shell speeds there is a substantial fraction of photons far in the wing of the line profile.

Table 1. Parameters of Models used in Figure 2.

#	σ (km s^{-1})	L_α (erg s^{-1})	$r_{\text{sh},i}$ (kpc)	$v_{\text{sh},i}$ (km s^{-1})	$N_{\text{HI},i}$ (cm^{-2})
1.	150	10^{43}	1.0	50	10^{20}
2.	150	10^{43}	1.0	150	10^{20}
3.	150	10^{43}	1.0	50	10^{19}

2.2 The Time Evolution of the Shell Speed: General Calculations

Given $f_{\text{scat}}(v_{\text{sh}}, N_{\text{HI}})$ we next use equation (1) to compute the evolution of the shell position (r_{sh}) and speed (v_{sh}) as follows:

1. The initial location and shell speed are denoted by $r_{\text{sh},i}$ and $v_{\text{sh},i}$. If the outflowing shell covers 4π steradians of the sky surrounding the Ly α emitting region (see Ahn 2004; Verhamme et al. 2008, for more detailed discussions), and if all the shell material is in neutral atomic hydrogen gas then $m_{\text{sh}} = 4\pi r_{\text{sh},i}^2 N_{\text{HI},i} m_p$, where r is the radius of the shell, $m_p = 1.6 \times 10^{-24} \text{ g}$ is the proton mass, and $N_{\text{HI},i}$ is the initial column density of neutral hydrogen atoms.
2. We combine equations (1) and (2) to compute dv_{sh}/dt .
3. Over an infinitesimal time step Δt a new shell position and velocity are then generated as $r_{\text{sh}}(t + \Delta t) = r_{\text{sh}}(t) + v_{\text{sh}}(t)\Delta t$ and $v_{\text{sh}}(t + \Delta t) = v_{\text{sh}}(t) + (dv_{\text{sh}}/dt)\Delta t$. At the new position, the shell's column density reduces to $N_{\text{HI}} = N_{\text{HI},i}(r_{\text{sh}}/r_{\text{sh},i})^{-2}$, and we return to step 2.

Our fiducial model has the following parameters. We adopt $\sigma = 150 \text{ km s}^{-1}$, corresponding to the circular virial velocity of a dark matter halo of mass $M = 10^{11} M_\odot$ at $z = 5.7$ as appropriate for a typical host of known Ly α emitting galaxies (e.g. Dijkstra et al. 2007). We also adopt $L_\alpha = 10^{43} \text{ erg s}^{-1}$, corresponding to the typical observed luminosity of Ly α emitting galaxies (e.g. Ouchi et al. 2007). This Ly α luminosity corresponds to a star formation rate of $\sim 5 M_\odot \text{ yr}^{-1}$ for a Salpeter IMF and a gas metallicity $Z = 0.05 Z_\odot$ (Schaerer 2003, for $Z = Z_\odot$ this star formation rate is higher by a factor of 2). For comparison, the total kinetic luminosity in supernova ejecta is $L_{\text{mech}} \sim 2 \times 10^{42} (E_{\text{mech}}/10^{51} \text{ erg}) (\mathcal{N}_{\text{SN}}/10^{-2}) \text{ erg s}^{-1}$, where \mathcal{N}_{SN} is the supernova rate per unit star formation rate, and E_{mech} is the total kinetic energy in ejecta per supernova explosion (e.g. Murray et al. 2005, and references therein).

For the shell, we assume $N_{\text{HI},i} = 10^{20} \text{ cm}^{-2}$, $r_{\text{sh},i} = 1.0 \text{ kpc}$ (see §1 and Verhamme et al. 2008) and $v_{\text{sh},i} = 50 \text{ km s}^{-1}$. We find that the final shell speed is not very sensitive to $v_{\text{sh},i}$. The above shell parameters imply a shell mass of $m_{\text{sh}} \sim 10^7 M_\odot$. The parameters of the fiducial model are summarized in Table 1.

The time evolution of the shell speed in the fiducial model is plotted as the *solid line* in the *left panel* of Figure 2, which shows that Ly α scattering accelerates the shell to $\sim 100 \text{ km s}^{-1}$ after 10 Myr, consistently with the crude estimate given in § 1. After 100 Myr, the shell speed reaches $\sim 230 \text{ km s}^{-1}$. The acceleration of the decreases with time because f_{scat} decreases with time. As the shell accelerates and expands, the fraction of Ly α photons that are scattered in the shell and the associated momentum transfer rate to the shell, decrease. Other lines in this panel represent models in which one of the model parameters was changed.

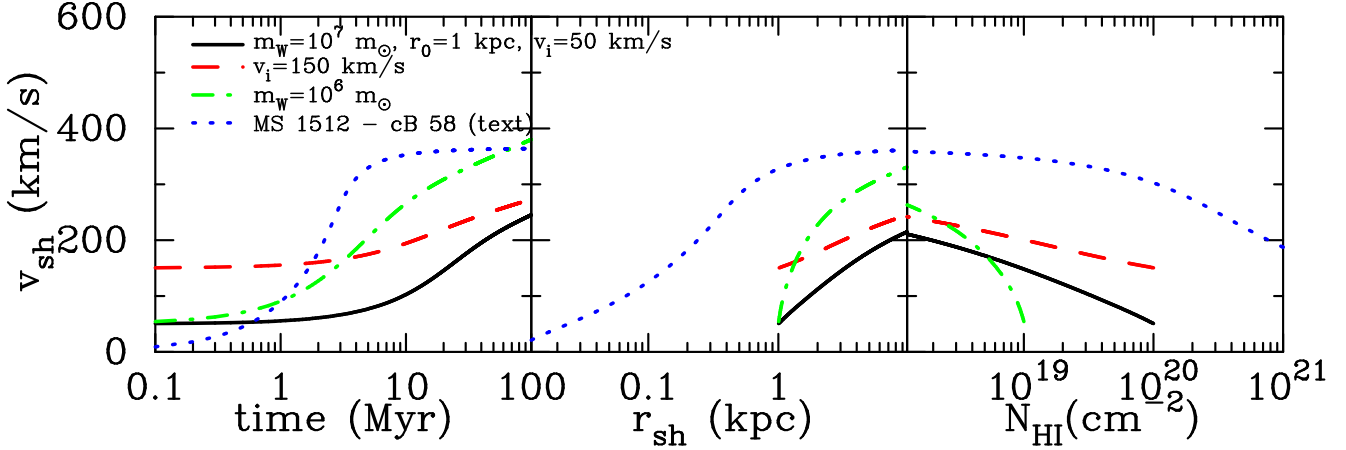


Figure 2. *Left panel:* Time evolution of the speed of an outflowing shell of neutral hydrogen that is accelerated by Ly α radiation from a star-forming galaxy. The *solid line* represents our fiducial model (see text and Table 1), in which Ly α scattering accelerates the shell to $\sim 100 \text{ km s}^{-1}$ in 10 Myr and to $\sim 230 \text{ km s}^{-1}$ in 100 Myr. Other curves represent models in which one of the model parameters was modified (except for the specific example illustrated by the *blue dotted line*; see § 2.3). The curves demonstrate that scattering of Ly α photons off an expanding shell can accelerate the shell to speeds that reach a few hundred km s^{-1} . *Central & Right panels* shows the shell velocity as a function of its radius & column density, respectively. In all examples except the dotted line, the shell starts at $r = 1 \text{ kpc}$ with a modest column density. In the model of LBG MS1512-cB58 (dotted line), the shell starts at $r = 10^{-2} \text{ kpc}$ with a higher column density that declines to the observed value as the shell expands (see text).

The *red dashed line* shows the shell evolution for a model in which the initial shell velocity was increased to $v_{\text{sh},i} = 150 \text{ km s}^{-1}$. The difference in shell speed between this case and the fiducial model decreases with time. In the model represented by the *green dot-dashed line* the shell mass is reduced to $m_{\text{sh}} = 10^6 M_{\odot}$ by reducing $N_{\text{HI},i}$. The shell speed evolves much faster, and reaches 200 km s^{-1} after $\sim 5 \text{ Myr}$. The final shell speed is $\sim 400 \text{ km s}^{-1}$. The *central (right) panel* shows the shell velocity as a function of its radius (column density). In the fiducial model (and those in which one parameter was changed), the shell started out at $r = 1 \text{ kpc}$ with a relatively low column density. The model represented by the *blue dotted lines* is discussed in § 2.3.

In all the above models, Ly α radiation pressure accelerates the shell up to a few hundreds of km s^{-1} . For comparison, the escape velocity from a halo with $v_{\text{circ}} = 150 \text{ km s}^{-1}$ (which corresponds to a mass of $3 \times 10^{11} [(1+z)/4]^{-3/2} M_{\odot}$, e.g. Barkana & Loeb 2001) for a shell starting at $r = 1 \text{ kpc}$ is $v_{\text{esc}} \sim 440 \text{ km s}^{-1}$ (at $z = 3$, with a very weak redshift dependence, see § 2.3). Therefore, it is reasonable to claim that shells that are driven by Ly α radiation pressure may escape from massive dark matter halos. Next we consider whether this mechanism could operate in known observed high-redshift LBGs that have measured values of L_{α} , N_{HI} and v_{sh} .

2.3 The Time Evolution of the Shell Speed in Known Galaxies

In real galaxies, Ly α radiation is not the only process that determines the shell kinematics, and Equation (1) modifies to

$$m_{\text{sh}} \frac{dv_{\text{sh}}}{dt} = f_{\text{scat}}(v_{\text{sh}}, N_{\text{HI}}) \frac{L_{\alpha}}{c} - F_{\text{grav}}(r) + 4\pi r^2 \Delta P, \quad (3)$$

where $F_{\text{grav}}(r)$ is the gravitational force on the shell, and $\Delta P = P_{\text{int}} - P_{\text{ext}}$ with $P = \rho c_s^2$ being the pressure of

the medium inside (“int”) or outside (“ext”) of the shell (Elmegreen & Chiang 1982). Here, ρ is the density of the medium, and c_s is its sound speed. The second and third terms on the right hand side of Eq. (3) require assumptions about the unknown shape of the gravitational potential near the star forming region and the local properties of the surrounding ISM.

To first order, gravity can be ignored in those galaxies for which the calculated terminal shell speed exceeds the escape velocity of the dark matter halo. More specifically, gravity can be ignored if the Ly α momentum transfer rate exceeds the gravitational force, $L_{\alpha}/c \gtrsim GM(< r_{\text{sh}})m_{\text{sh}}/r_{\text{sh}}^2$, where $M(< r_{\text{sh}})$ is the total mass enclosed by the supershell. Quantitatively, Ly α radiation pressure exceeds gravity when the Ly α luminosity exceeds

$$L_{\alpha} \gtrsim 10^{43} \text{ erg s}^{-1} \left(\frac{M(< r_{\text{sh}})}{10^8 M_{\odot}} \right) \left(\frac{m_{\text{sh}}}{10^6 M_{\odot}} \right) \left(\frac{r_{\text{sh}}}{0.1 \text{ kpc}} \right)^{-2}. \quad (4)$$

If the radial density profile can be modeled as an isothermal sphere, then $M(< r_{\text{sh}}) \sim M_{\text{tot}}(r_{\text{sh}}/r_{\text{vir}})$ and the required luminosity increases at smaller shell radii. However, if the shell starts at a small radius (i.e. $r_{\text{sh},i} = 0.01 \text{ kpc}$), then for a fixed shell mass the column density is high (e.g. $N_{\text{HI},i} \gg 10^{22} \text{ cm}^{-2}$). This, in combination with the small initial velocity of the shell, implies that the Ly α photons are efficiently trapped and the impact of radiation pressure is bigger than estimated above (see Fig. 3 and Paper I). In Paper I we showed that in this regime, a simple order-of-magnitude estimate for the importance of radiation pressure is obtained based on energy considerations (e.g. Cox 1985; Bithell 1990; Oh & Haiman 2002). Initially, the total gravitational binding energy of the shell is $|U_{\text{sh}}| = GM(< r_{\text{sh},i})m_{\text{sh}}/r_{\text{sh},i}$. The energy in the Ly α radiation field is $U_{\alpha} = L_{\alpha} t_{\text{trap}}$, where t_{trap} is the typical trapping time of a Ly α photon in the neutral shell. The trapping time scales with the shell optical depth at the Ly α line center, τ_0 , through the relation $t_{\text{trap}} \sim 15(\tau_0/10^{5.5})r_{\text{sh},i}/c$ (Adams 1975; Bonilha et al.

1979). Radiation pressure unbinds the gas when $U_\alpha > |U_{\text{sh}}|$. We find this to be the case for all galaxies discussed below (except the first model of FDF 1267). Also $U_\alpha \gg |U_{\text{sh}}|$ for those galaxies in which the calculated terminal wind speed exceeds the escape velocity of the halo, which confirms that ignoring gravity is justified best for those galaxies in which the Ly α radiation pressure can accelerate the shell to a speed that exceeds the escape velocity of the host dark matter halo.

Since we investigate the properties of Ly α -driven supershells, we assume that ΔP is less than the Ly α radiation pressure (this assumption is motivated by the possibility that Ly α radiation pressure provides the dominant source of pressure on neutral hydrogen gas in the ISM, see § 1 and Paper I). Hence, we solve Eq. 3 under the assumption that the second and third terms on its right hand side can be ignored. We initiate a shell at rest ($v_{\text{sh},i} = 0$) at a very small radius ($r_{\text{sh},i} = 0.01$ kpc, and not at the origin to avoid a divergent $N_{\text{HI},i} \rightarrow \infty$). We get constraints on the mass, age and radius of the supershell by requiring that it reaches its observed expansion velocity at its observed column density (see § 2.3.1 for an example).

Our results are summarized in Table 2. The first column contains the name of the galaxy. The second column contains the HI column density and the third contains the shell speed as derived from fitting to the observed Ly α line profile (Schaerer & Verhamme 2008; Verhamme et al. 2008). The fourth column contains the *intrinsic* Ly α luminosity, which was inferred from the UV-based star formation rate, and the *intrinsic* Ly α equivalent width derived by Schaerer & Verhamme (2008) and Verhamme et al. (2008), as³ $L_\alpha \sim (\text{SFR}/M_\odot/\text{yr}) \times (\text{EW}_{\text{int}}/70 \text{ \AA}) \times 10^{42} \text{ erg s}^{-1}$ (e.g. Dijkstra & Wyithe 2007). The radius (r_{sh}), angular scale on the sky (θ_α), mass (m_{sh}), and age (t_{sh}) of the supershell are given in the fifth, sixth, seventh, and eighth columns, respectively. The ninth column contains the energy of the supershell, which is given by $E_{\text{sh}} = \frac{1}{2} m_{\text{sh}} v_{\text{sh}}^2$. The tenth column gives the asymptotic (terminal) shell speed, to be compared with the escape velocity of the galaxy in the eleventh column. For an isothermal sphere, the escape velocity relates to the circular velocity as $v_{\text{esc}} = \sqrt{2} v_{\text{circ}} \sqrt{\ln[r_{\text{vir}}/r_{\text{sh},i}]}$ (see Eqs. (2-25), (4-117) & (4-123) of Binney & Tremaine 1987, and Eqs. (24) & (25) of Barkana & Loeb 2001). The circular velocity v_{circ} was obtained from $v_{\text{circ}} = \text{FWHM}/2.35$, in which 'FWHM' is the intrinsic Full Width at Half Maximum of the Ly α line quoted by Verhamme et al. (2008, see e.g. Dijkstra et al. 2007 for a more extended discussion on this relation). The twelfth column contains a fudge factor f which is defined as $f \equiv r_{\text{sh}}/(\frac{1}{2} \tilde{a}_{\text{sh}} \tilde{r}_{\text{sh}}^2)$, where $\tilde{a}_{\text{sh}} \equiv L_\alpha/cm_{\text{sh}}$, and $\tilde{r}_{\text{sh}} \equiv 2r_{\text{sh}}/v_{\text{sh}}$ (i.e. $f = 1$ for $f_{\text{scat}} = 1$, and $f < 1$ when $f_{\text{scat}} < 1$). The radius of the shell can then be expressed as a function of the observed quantities L_α , N_{HI} , and v_{sh} as

$$r_{\text{sh}} = \frac{f}{2\pi\mu m_p c} \frac{L_\alpha}{N_{\text{HI}} v_{\text{sh}}^2} \quad (5)$$

Finally, the thirteenth column contains the ratio between the mass outflow rate in the supershell given by $\dot{M} = 6.0 \times (r_{\text{sh}}/1 \text{ kpc}) (N_{\text{HI}}/10^{20} \text{ cm}^{-2}) (v_{\text{sh}}/200 \text{ km s}^{-1}) M_\odot$

yr^{-1} (Verhamme et al. 2008), and the UV-derived star formation rate (in $M_\odot \text{ yr}^{-1}$).

Throughout our calculations of f_{scat} we have used the b -parameter similarly to Schaerer & Verhamme (2008) and Verhamme et al. (2008) instead of v_{th} , i.e. we substituted $\Delta\nu_D = b\nu_\alpha/c$ in equation (2). Below, we describe individual cases in more detail.

2.3.1 MS1512-cB58

Pettini et al. (2002) have found that the lensed Lyman Break galaxy (LBG) MS1512-cB58 is surrounded by an outflowing shell of gas with a column density $N_{\text{HI}} = 7.5 \times 10^{20} \text{ cm}^{-2}$, which is expanding at a speed of $v_{\text{sh}} = 200 \text{ km s}^{-1}$ (also see Schaerer & Verhamme 2008). The star formation rate inside the LBG, $\sim 40 M_\odot \text{ yr}^{-1}$, translates to an intrinsic Ly α luminosity of $\sim 4\text{--}8 \times 10^{43} \text{ erg s}^{-1}$ (with the uncertainty due to the unknown metallicity of the gas, see Schaerer 2003). We adopt the central value of $L_\alpha = 6 \times 10^{43} \text{ erg s}^{-1}$.

The *blue dotted line* in Figure 2 depicts the time evolution of a shell with $m_{\text{sh}} = 3 \times 10^6 M_\odot$ and the above parameters of MS1512-cB58. The plot shows that the observed shell velocity is reached at $t \sim 1.9 \text{ Myr}$, when the shell reaches a radius $r = 0.21 \text{ kpc}$ and has an observed column density of $N_{\text{HI}} = 7.5 \times 10^{20} \text{ cm}^{-2}$. More massive shells would reach the observed speed at later times, larger radii, and at a lower shell column density. The plot also shows that Ly α pressure accelerates the shell to $\sim 360 \text{ km s}^{-1}$ after 10 Myr, at which point the column density has declined to $\sim 4 \times 10^{18} \text{ cm}^{-2}$.

Lastly, we point that the HI shell in MS1512-cB58 is known to contain dust, with an estimated extinction of $E(B - V) \sim 0.3$ (Schaerer & Verhamme 2008, and references therein), which implies an approximate optical depth at 1216 Å of $\tau_D \sim 1.8 - 3.3$ (e.g. Verhamme et al. 2008). We argue in § 3 that despite the presence of this dust, the Ly α radiation pressure can still be substantial (and possibly dominant over continuum radiation pressure).

2.3.2 Ly α Emitters in the FORS Deep Field

Verhamme et al. (2008) reproduced the observed Ly α line profiles of 11 LBGs from the FORS Deep Field at $2.8 \lesssim z \lesssim 5$ observed by Tapken et al. (2007) based on a simple model in which the Ly α photons emitted by the LBGs backscatter off a single spherical outflowing shell with $2 \times 10^{19} \text{ cm}^{-2} \lesssim N_{\text{HI}} \lesssim 7 \times 10^{20} \text{ cm}^{-2}$.

Table 2 contains two entries for FDF 1267 because two different models were found to reproduce the observed line profile. We have not included galaxies FDF 4691 and FDF 7539 in the table because these galaxies contained almost static supershells, which cannot be reproduced by our approach, possibly because the shells in these galaxies were slowed down by gravity.

For several galaxies our model can be ruled out: our predicted r_{sh} for FDF 4691 exceeds the size of the largest observed Ly α emitting structure in our Universe, which is $\sim 150 \text{ kpc}$ in diameter (Steidel et al. 2000). Furthermore, we find ages of $t_{\text{sh}} \sim 0.1 \text{ Myr}$ for two galaxies (FDF 5215 and FDF 1267). While this is not physically impossible, it appears unlikely that we have caught star forming regions

³ This implies that we convert a rest-frame UV luminosity density into a Ly α luminosity using only the intrinsic EW given by Verhamme et al. (2008). The actual star formation rates that are associated with these UV luminosity densities are irrelevant.

Table 2. Predicted physical sizes of expanding HI supershells under the assumption that *their expansion was driven predominantly by Ly α radiation pressure*.

Galaxy name	N_{HI} ($10^{20}/\text{cm}^2$)	v_{sh} (km/s)	L_{α} ($10^{43} \frac{\text{erg}}{\text{s}}$)	r_{sh} (kpc)	θ_{α} ($''$)	m_{sh} ($10^6 M_{\odot}$)	t_{sh} (Myr)	E_{sh} (10^{54} erg)	v_{term} (km/s)	v_{esc} (km/s)	f	$\frac{\dot{M}}{\text{SFR}}$
cB-58	7.5	200.	6.	0.22	0.03	3.3	1.9	1.3	370	134	1.0	0.24
FORS Deep Field Galaxies observed by Tapken et al (2007). Parameters taken from Verhamme et al (2008).												
1267	0.2	50.	0.3	5.5	0.69	58	200	1.4	110.	544	0.85	1.4
1267	3	300.	1.	0.03	0.004	0.03	0.14	0.02	544	170	1.0	0.7
1337	5	200.	2.5	0.12	0.016	0.7	1.05	0.27	437	170	0.89	0.1
2384	0.3	150.	5.	7.4	1.0	157	89	35	164	170	0.92	0.4
3389	0.2	150.	1.2	2.5	0.37	12	29.5	2.7	210	263	0.87	0.2
4454	0.2	150.	0.28	0.63	0.8	0.08	7.4	0.2	211	256	0.92	0.3
5215	7	400.	4.4	0.03	0.004	0.06	0.1	0.1	780	170	0.65	0.1
5550	5	200.	4.2	0.21	0.03	2	1.9	0.84	430	170	0.93	0.1
5812	0.2	150.	2.0	4.3	0.67	35	50	8	196	165	0.90	0.7
6557	0.4	150.	1.4	1.7	0.26	11	22	2.5	223.	166	1.0	0.2
4691	0.8	10	18	230	30	4×10^5	4×10^4	400	-	1936	0.83	3.9
7539	5.0	25	42	15	2.0	10^4	10^3	67	-	170	1.0	1.9

that early in their evolution. Indeed, these predicted ages fall well below the plausible age range that was derived for local supershells. Lastly, we predict a radius $r_{\text{sh}} = 15$ kpc for FDF 7531. Our model therefore predicts that existing observations should have resolved this galaxy as a spatially extended Ly α source (which is not observed).

For most other galaxies, $r_{\text{sh}} \sim 0.1$ – 10 kpc, $t_{\text{sh}} \sim 1$ – 200 Myr, and $E_{\text{sh}} \sim 10^{53}$ – 10^{55} ergs. For comparison, McClure-Griffiths et al. (2002) find $r_{\text{sh}} \sim 0.07$ – 0.7 kpc, $t_{\text{sh}} \sim 0.9$ – 20 Myr, and $E_{\text{sh}} = 0.03$ – 5×10^{53} ergs for 19 galactic supershells. Our largest shells are larger than those of supershells that were observed in our galaxy, but are comparable in size of the inferred sizes of HI outflows around local star burst galaxies (Mass-Hesse et al. 2003). Thus, there is considerable overlap in the physical properties of observed (extra)galactic supershells and those in our model, although our model does contain a few supershells that are significantly larger and more energetic than observed galactic supershells. This may be because we ignore gravity. Indeed, for these energetic shells ($E_{\text{sh}} \gtrsim$ a few 10^{54} erg), the maximum shell speed does not exceed the escape velocity of the host dark matter halo, and so gravity cannot be ignored.

We caution that the escape velocity of the dark matter halo that we computed are approximate. Our escape velocity was derived using the relation $v_{\text{esc}} = \sqrt{2}v_{\text{circ}}\sqrt{\ln[r_{\text{vir}}/r_{\text{sh},i}]}$, which assumes that the shell climbs out of the gravitational potential of an isothermal sphere⁴. Although our calculated v_{esc} depends only weakly on $r_{\text{sh},i}$, we caution that deviations from our assumed simple model may change the results somewhat.

Interestingly, the fudge factor f is within the range 0.65 – 1.0 in all models. The small scatter in f arises because all shells initially have much higher HI column densities than

their observed values. Therefore, for all shells the parameter $f_{\text{scat}} = 1$ during the early stages of their evolution. Depending on the precise time evolution of column density and shell speed, f_{scat} eventually drops below unity (for some galaxies this has not happened yet and $f_{\text{scat}} = 1$, which in turn implies $f = 1$). Additional scatter may arise from the fact that some shells have predicted size that are close to the initial shell size assumed for our models.

The small scatter in f implies that one can predict physical properties of galactic supershells without numerically integrating equation (3). Instead, one may simply adopt the central value $f \sim 0.9$ and apply Eq. (5) to quantities such as L_{α} , N_{HI} and v_{sh} to predict r_{sh} . We also find that the mass outflow rates in supershells reach ~ 10 – 100% of the star formation rates in their host galaxies, consistently with the *total* outflow rates that one expects theoretically (e.g. Erb 2008).

3 DISCUSSION & CONCLUSIONS

It is well known that scattering of Ly α photons by neutral hydrogen in a single outflowing supershell around star-forming galaxies can naturally explain two observed phenomena: (i) the common shift of the Ly α emission line towards the red relative to other nebular recombination and metal absorption lines, and (ii) the asymmetry of the Ly α line with emission extending well into its red wing. In this paper we have computed the radiation pressure that is exerted by this scattered Ly α radiation on the outflowing shell.

We have shown that for reasonable shell parameters the shell can be accelerated to a few hundred km s^{−1} after $\lesssim 10$ Myr. The Ly α acceleration mechanism becomes increasingly inefficient as the shell speed increases (Fig. 1), because the Doppler boost of the gas extends increasingly farther into the wing of the Ly α absorption profile allowing a decreasing fraction of the Ly α photons to scatter on the outflowing shell. Furthermore, for a shell mass that is constant in time, $N_{\text{HI}} \propto r^{-2}$, and we find that for any choice of model parameters the shell achieves a terminal velocity that depends

⁴ The isothermal sphere model for the inner mass distribution of galaxies is supported observationally by gravitational lensing studies of elliptical galaxies (e.g. Winn et al. 2003; Bolton et al. 2008) and by the observed flatness of the rotation curves of spiral galaxies (e.g. Begeman 1989; Sanders & McGaugh 2002)

mainly⁵ on its total mass and the Ly α luminosity of the central source (Fig. 2).

We have computed the physical properties of expanding supershells that are likely to be present in specific observed high-redshift ($z = 2.7\text{--}5.0$) galaxies, under the assumptions that they are driven predominantly by Ly α radiation pressure and that their mass remains constant in time. We predict supershell radii that lie in the range $r_{\text{sh}} = 0.1\text{--}10$ kpc, ages in the range $t_{\text{sh}} = 1\text{--}100$ Myr, and energies in the range $E_{\text{sh}} = 10^{53}\text{--}10^{55}$ ergs, in broad agreement with the properties of local galactic supershells. We derive mass outflow rates in the supershells that reach $\sim 10\text{--}100\%$ of the star formation rates in the host galaxies, in agreement with the *total* outflow rates that one expects theoretically (e.g. Erb 2008).

We have found that in all models the radius of the supershell is determined uniquely by parameters such as the *intrinsic* Ly α luminosity of the host galaxy (which may be inferred from the observed Ly α line shape), L_{α} , the total column density of HI in the supershell, N_{HI} , and the shell velocity v_{sh} ,

$$\left(\frac{r_{\text{sh}}}{\text{kpc}}\right) \sim 0.2 \left(\frac{f}{0.9}\right) \left(\frac{L_{\alpha}}{10^{43} \frac{\text{erg}}{\text{s}}}\right) \left(\frac{10^{20}/\text{cm}^2}{N_{\text{HI}}}\right) \left(\frac{200 \frac{\text{km}}{\text{s}}}{v_{\text{sh}}}\right)^2. \quad (6)$$

Here f is a fudge factor that lies in the range $f = 1.0\text{--}1.3$. Our models have ignored gravity and the pressure of exerted by the surrounding interstellar medium. *This relation holds up only for supershells that are driven predominantly by Ly α radiation pressure.* This relation is most accurate for those galaxies in which the shells are accelerated to velocities that exceed v_{esc} . We found this to be the case in 5 out of 9 (55%, see Table 2, ignoring the galaxies for which our model was ruled out, i.e. FDF 1267b, FDF 5215, FDF 4691, and FDF 7539) of known galaxies. Hence, these shells could contribute to the enrichment of the intergalactic medium.

In other cases, gravity (and external pressure) will tend to reduce the value of the fudge factor f . Also, if neutral hydrogen gas only makes up a fraction f_{HI} of the total mass of the shell (see § 1), then our predicted value of r_{sh} should be lowered by a factor of f_{HI} .

On the other hand, as was already mentioned in § 2, our conservative calculations have completely ignored the fact that ‘trapping’ of Ly α radiation by the optically thick supershell may significantly boost the Ly α radiation pressure compared to what was used in this paper. Specifically, it was shown in Paper I that when this trapping is properly accounted for, the total radiation force in Eq. 1 should include $M_F(v_{\text{sh}}, N_{\text{HI}})$ in place of $f_{\text{scat}}(v_{\text{sh}}, N_{\text{HI}})$. Here, M_F is ‘force-multiplication’ factor⁶ that depends both the column

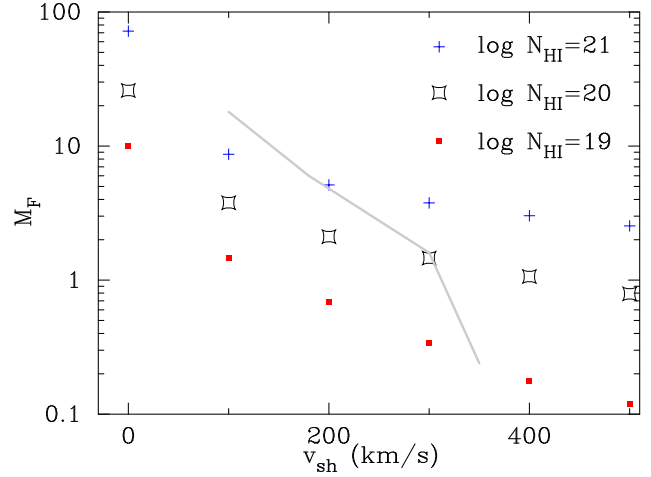


Figure 3. When Ly α trapping is properly accounted for, the total radiation force in Eq. 1 should be modified as $f_{\text{scat}}(v_{\text{sh}}, N_{\text{HI}}) \rightarrow M_F(v_{\text{sh}}, N_{\text{HI}})$. Here, we plot M_F (a ‘force-multiplication’ factor) as a function of the expansion velocity of the HI shell, v_{sh} , for three values of HI column density. M_F was calculated by performing Monte-Carlo Ly α radiative transfer calculation (described in Paper I), and under the assumption that the HI shell surrounds an empty cavity. M_F increases with increasing N_{HI} and decreasing v_{sh} . The *grey line* is the trajectory in the $N_{\text{HI}} - v_{\text{sh}}$ plane of the model of the supershell in cB-58 (§ 2.3.1). Clearly, especially at early times we have underestimated the radiation pressure force significantly, which renders our calculations conservative.

density of HI and the velocity of the supershell. In Paper I, M_F was computed for a range of N_{HI} and v_{sh} values, by performing Monte-Carlo Ly α radiative transfer calculation for each combination of N_{HI} and v_{sh} . In these calculations, the HI shell surrounds an empty cavity. The results of these calculations are shown in Fig. 3. As evident from the plot, M_F greatly exceeds unity for low shell velocities and large HI column densities. Overplotted as the *grey line* is the trajectory in the $N_{\text{HI}} - v_{\text{sh}}$ plane of the supershell in cB-58 (§ 2.3.1). At early times, $M_F > 10$, and we may have underestimated the radiation pressure force significantly (as was mentioned in § 2, the actual force multiplication factor may be less than M_F , if gas and dust interior to the supershell prevents photons from repeatedly ‘bouncing’ back and forth between opposite sides of the HI shell). Ly α trapping could boost our predicted value of r_{sh} by a factor as large as $\langle M_F \rangle$, where $\langle M_F \rangle$ the value of M_F , averaged over the expansion history of the shell.

So far, we have assumed HI to be the only source of opacity in the supershell. However, supershells may also contain dust which provides an additional source of opacity; for example, in the models of Verhamme et al (2008), the optical depth through dust at $\lambda = 1216$ Å is $\tau_{\text{D}} = 0.0\text{--}2.0$. At a given HI column density, we have therefore systematically underestimated f_{scat} , (absorption of a Ly α photon by dust also results in a momentum transfer of magnitude $h\nu_{\alpha}/c$), which renders our calculations conservative. Furthermore,

$M(t)$ arises because of the contribution of numerous metal absorption lines to the medium’s opacity, and can be as large as $M_{\text{max}}(t) \sim 10^3$ in the atmospheres of O-stars (Castor et al. 1975).

⁵ An alternative way to see why the observed quantities N_{HI} , v_{sh} , and L_{α} provide unique constraints on the shell mass, radius, and age is that these three unknown quantities relate to the observed quantities via three equations: 1. $m_{\text{sh}} = 4\pi r_{\text{sh}}^2 N_{\text{HI}} \mu_p$ and 2. $v_{\text{sh}} \sim \frac{L_{\alpha}}{cm_{\text{sh}}} t_{\text{sh}}$, and 3. $r_{\text{sh}} \sim \frac{L_{\alpha}}{2cm_{\text{sh}}} t_{\text{sh}}^2$. We found that Equations 2. and 3. are accurate to within $\sim 50\%$.

⁶ This term derives from the (time-dependent) force-multiplication function $M(t)$ that was introduced by Castor et al. (1975), as $F_{\text{rad}} \equiv M(t) \frac{\tau_e L_{\text{bol}}}{c}$. Here, F_{rad} is the total force that radiation exerts on a medium, τ_e is the total optical depth to electron scattering through this medium. The function

dusty supershells could also absorb significant amounts of continuum radiation, boosting the total momentum transfer rate even further. If the dust resides interior to the HI shell, then the Ly α flux that impinges upon the shell is reduced by $e^{-\tau_d(\lambda_\alpha)}$. In this case, the Ly α (as well as the continuum) radiation pressure is smaller than computed in this paper. However, the coupling between gas and dust makes it very unlikely that (Ly α) radiation pressure sweeps up the gas surrounding a star forming region, while keeping the dust in place (see Murray et al. 2005, for more discussion on this).

Of course, the existence of dust inside the HI shell reduces its ability to 'trap' Ly α photons, which reduces the value of M_F compared to that shown in Figure 3. Despite this reduction, M_F can still greatly exceed unity, because at low shell expansion velocities the majority of Ly α photons do not penetrate deeply into the HI shell upon their first entry. Instead, the photons mostly scatter near the surface of the shell, and only 'see' a fraction of the dust opacity (indeed, for this reason Ly α radiation can escape from a dusty two-phased ISM, see Neufeld 1991 and Hansen & Oh 2006). In other words, a relative small inner portion the HI shell can effectively trap Ly α photons. We have verified this statement with Monte-Carlo radiative transfer calculations that included dust at the levels inferred by Verhamme et al. (2008): we typically found M_F to be reduced by a factor of up to a few. In other words, even for dusty shells it is possible that $M_F \gg 1$.

Therefore, the pressure exerted by Ly α radiation alone can exceed the maximum possible pressure exerted by continuum radiation (also see Paper I), which can drive the large gas masses (as large as a few $10^{10-11} M_\odot$) out of galaxies in a galactic *superwind* (Murray et al. 2005). For comparison, in our model the Ly α photons transfer their momentum onto the expanding supershell, which contains significantly less mass ($m_{\text{sh}} \lesssim 10^8 M_\odot$). This implies that in principle, both mechanisms could operate simultaneously, and that the neutral HI supershells may be accelerated to higher velocities than the bulk of the ejected gas. Since in our model Ly α radiation pressure operates only on a fraction of the gas, it does not provide a self-regulating mechanism for star formation and black hole growth as in Murray et al. (2005). However, it does provide a new way of enriching the intergalactic medium with metals.

We note that quasars can have Ly α luminosities⁷ that reach $L_\alpha = 10^{46} \text{ erg s}^{-1}$ (Fan et al. 2006). In principle, this Ly α luminosity could transfer a significant amount of momentum onto neutral gas in its proximity. Because the Ly α emission line of quasars is typically very broad (\sim few thousand km s^{-1}), f_{scat} is significantly less than unity for the column densities considered in the paper (see Fig. 1). Furthermore, it is unclear whether gas clouds can remain neutral in close proximity to the quasar for an extended period of time. Even if this is the case, it remains to be determined whether the Ly α radiation pressure can compete with the continuum radiation pressure. The importance of Ly α radiation pressure near quasars therefore remains an open issue.

⁷ Empirically, the Ly α luminosity of quasars is related to their B-band luminosity as $L_\alpha \sim 0.7 L_B$ (Dijkstra & Wyithe, 2006). High-redshift quasars have been observed with $L_B \gtrsim 10^{13} L_{B,\odot} = 4 \times 10^{45} \text{ erg s}^{-1}$ (see e.g. Figure 1 of Dijkstra & Wyithe, 2006).

To conclude, observations indicate that it is the kinematics of HI gas surrounding star forming regions that mostly determines the observed properties of the Ly α radiation (as opposed to dust content, e.g. Kunth et al. 1998; Atek et al. 2008; Hayes et al. 2008; Ostlin et al. 2008). This work suggests that -at least in some cases- the pressure exerted by the Ly α photons themselves may be important in determining the kinematics of HI gas. This is appealing for two reasons: (i) the mechanism operates irrespective of the dust content of the HI supershells. This mechanism may therefore operate also in galaxies of primordial composition at high redshift (especially since the total Ly α luminosity per unit star formation rate is higher, e.g. Schaerer 2003), and (ii) the shape and velocity offset of the observed Ly α emission strongly suggest that momentum transfer from Ly α photons to HI gas is actually observed to occur.

Acknowledgments This work is supported by in part by NASA grant NNX08AL43G, by FQXi, and by Harvard University funds. We thank an anonymous referee for constructive comments that improved the presentation of this paper.

REFERENCES

- Adams, T. F. 1975, ApJ, 201, 350
- Ahn, S.-H., Lee, H.-W., & Lee, H. M. 2002, ApJ, 567, 922
- Ahn, S.-H., & Lee, H.-W. 2002, Journal of Korean Astronomical Society, 35, 175
- Ahn, S.-H., Lee, H.-W., & Lee, H. M. 2003, MNRAS, 340, 863
- Ahn, S.-H. 2004, ApJL, 601, L25
- Atek, H., Kunth, D., Hayes, M., Å-Stlin, G., & Mas-Hesse, J. M. 2008, A&A,
- Barkana, R., & Loeb, A. 2001, Physics Reports, 349, 125
- Begeman, K. G. 1989, A&A, 223, 47
- Binney, J., & Tremaine, S. 1987, Princeton, NJ, Princeton University Press, 1987, 747 p.,
- Bithell, M. 1990, MNRAS, 244, 738
- Bolton, A. S., Treu, T., Koopmans, L. V. E., Gavazzi, R., Moustakas, L. A., Burles, S., Schlegel, D. J., & Wayth, R. 2008, ArXiv e-prints, 805, arXiv:0805.1932
- Bonilha, J. R. M., Ferch, R., Salpeter, E. E., Slater, G., & Noerdlinger, P. D. 1979, ApJ, 233, 649
- Castor, J. I., Abbott, D. C., & Klein, R. I., 1975, ApJ, 195, 157
- Cox, D. P. 1985, ApJ, 288, 465
- Dijkstra, M. & Wyithe, J. Stuart B. 2006, MNRAS, 372, 1575
- Dijkstra, M., Lidz, A., & Wyithe, J. S. B. 2007, MNRAS, 377, 1175
- Dijkstra, M., & Wyithe, J. S. B. 2007, MNRAS, 379, 1589
- Dijkstra, M., & Loeb, A. 2008, Accepted for publication in MNRAS(Paper I), arXiv:0807.2645
- Dunkley, J., et al. 2008, ArXiv e-prints, 803, arXiv:0803.0586
- Elmegreen, B. G., & Chiang, W.-H. 1982, ApJ, 253, 666
- Erb, D. K. 2008, ApJ, 674, 151
- Fan, X., et al. 2006, AJ, 132, 117
- Furlanetto, S. R., & Loeb, A. 2003, ApJ, 588, 18
- Hansen, M., & Oh, S. P. 2006, MNRAS, 367, 979

- Hayes, M., Ostlin, G., Mas-Hesse, J. M., & Kunth, D. 2008, ArXiv e-prints, 803, arXiv:0803.1176
- Heckman, T. M., Armus, L., & Miley, G. K. 1990, ApJS, 74, 833
- Heiles, C. 1984, ApJS, 55, 585
- Ivezic, Z., & Elitzur, M. 1995, ApJ, 445, 415
- Komatsu, E., et al. 2008, ArXiv e-prints, 803, arXiv:0803.0547
- Martin, C. L. 1999, ApJ, 513, 156
- Kunth, D., Mas-Hesse, J. M., Terlevich, E., Terlevich, R., Lequeux, J., & Fall, S. M. 1998, A&A, 334, 11
- Lee, H.-W., & Ahn, S.-H. 1998, ApJL, 504, L61
- Lequeux, J., Kunth, D., Mas-Hesse, J. M., & Sargent, W. L. W. 1995, A&A, 301, 18
- Martin, C. L. 1999, ApJ, 513, 156
- Martin, C. L. 2005, ApJ, 621, 227
- Mas-Hesse, J. M., Kunth, D., Tenorio-Tagle, G., Leitherer, C., Terlevich, R. J., & Terlevich, E. 2003, ApJ, 598, 858
- McClure-Griffiths, N. M., Dickey, J. M., Gaensler, B. M., & Green, A. J. 2002, ApJ, 578, 176
- McClure-Griffiths, N. M., Ford, A., Pisano, D. J., Gibson, B. K., Staveley-Smith, L., Calabretta, M. R., Dedes, L., & Kalberla, P. M. W. 2006, ApJ, 638, 196
- Murray, N., Quataert, E., & Thompson, T. A. 2005, ApJ, 618, 569
- Neufeld, D. A. 1991, ApJL, 370, L85
- Oh, S. P., & Haiman, Z. 2002, ApJ, 569, 558
- Ostlin, G., Hayes, M., Kunth, D., Mas-Hesse, J. M., Leitherer, C., Petrosian, A., & Atek, H. 2008, ArXiv e-prints, 803, arXiv:0803.1174
- Ouchi, M., et al. 2007, ArXiv e-prints, 707, arXiv:0707.3161
- Partridge, R. B., & Peebles, P. J. E. 1967, ApJ, 147, 868
- Pettini, M., Steidel, C. C., Adelberger, K. L., Dickinson, M., & Giavalisco, M. 2000, ApJ, 528, 96
- Pettini, M., Shapley, A. E., Steidel, C. C., Cuby, J.-G., Dickinson, M., Moorwood, A. F. M., Adelberger, K. L., & Giavalisco, M. 2001, ApJ, 554, 981
- Pettini, M., Rix, S. A., Steidel, C. C., Adelberger, K. L., Hunt, M. P., & Shapley, A. E. 2002, ApJ, 569, 742
- Ryder, S. D., Staveley-Smith, L., Malin, D., & Walsh, W. 1995, AJ, 109, 1592
- Salpeter, E. E. 1974, ApJ, 193, 585
- Sanders, R. H., & McGaugh, S. S. 2002, ARA&A, 40, 263
- Santos, M. R. 2004, MNRAS, 349, 1137
- Schaerer, D. 2003, A&A, 397, 527
- Schaerer, D., & Verhamme, A. 2008, A&A, 480, 369
- Steidel, C. C., Adelberger, K. L., Shapley, A. E., Pettini, M., Dickinson, M., & Giavalisco, M. 2000, ApJ, 532, 170
- Shapley, A. E., Steidel, C. C., Pettini, M., & Adelberger, K. L. 2003, ApJ, 588, 65
- Tapken, C., Appenzeller, I., Noll, S., Richling, S., Heidt, J., Meinköhn, E., & Mehlert, D. 2007, A&A, 467, 63
- Tenorio-Tagle, G., & Bodenheimer, P. 1988, ARA&A, 26, 145
- Tenorio-Tagle, G., Silich, S. A., Kunth, D., Terlevich, E., & Terlevich, R. 1999, MNRAS, 309, 332
- Verhamme, A., Schaerer, D., & Maselli, A. 2006, A&A, 460, 397
- Verhamme, A., Schaerer, D., Atek, H., & Tapken, C. 2008, ArXiv e-prints, 805, arXiv:0805.3601
- Winn, J. N., Rusin, D., & Kochanek, C. S. 2003, ApJ, 587,